

Characterization of cell surface and extracellular matrix remodeling of *Azospirillum brasilense* chemotaxis-like 1 signal transduction pathway mutants by atomic force microscopy

Amanda Nicole Edwards^{1,2}, Piro Siuti^{1,2}, Amber N. Bible³, Gladys Alexandre^{2,3}, Scott T. Retterer^{1,4}, Mitchel J. Doktycz^{1,2,4} & Jennifer L. Morrell-Falvey^{1,2}

¹Oak Ridge National Laboratory, Biosciences Division, Oak Ridge, TN, USA; ²Oak Ridge National Laboratory, Graduate School of Genome Science and Technology, University of Tennessee, Knoxville, TN, USA; ³Department of Biochemistry, Cellular and Molecular Biology, University of Tennessee, Knoxville, TN, USA; and ⁴Oak Ridge National Laboratory, Center for Nanophase Materials Sciences, Oak Ridge, TN, USA

Correspondence: Jennifer L. Morrell-Falvey, Oak Ridge National Laboratory, Biosciences Division, Oak Ridge, TN 37831, USA.
Tel.: +1 865 241 2841; fax: +1 865 574 5345;
e-mail: morrelljl1@ornl.gov

Received 18 October 2010; accepted 24 October 2010.
Final version published online 24 November 2010.

DOI:10.1111/j.1574-6968.2010.02156.x

Editor: Yaacov Okon

Keywords

flocculation; *Azospirillum brasilense*; CheY; CheA; exopolysaccharide; lipopolysaccharides.

Abstract

To compete in complex microbial communities, bacteria must sense environmental changes and adjust cellular functions for optimal growth. Chemotaxis-like signal transduction pathways are implicated in the regulation of multiple behaviors in response to changes in the environment, including motility patterns, exopolysaccharide production, and cell-to-cell interactions. In *Azospirillum brasilense*, cell surface properties, including exopolysaccharide production, are thought to play a direct role in promoting flocculation. Recently, the Che1 chemotaxis-like pathway from *A. brasilense* was shown to modulate flocculation, suggesting an associated modulation of cell surface properties. Using atomic force microscopy, distinct changes in the surface morphology of flocculating *A. brasilense* Che1 mutant strains were detected. Whereas the wild-type strain produces a smooth mucosal extracellular matrix after 24 h, the flocculating Che1 mutant strains produce distinctive extracellular fibril structures. Further analyses using flocculation inhibition, lectin-binding assays, and comparison of lipopolysaccharides profiles suggest that the extracellular matrix differs between the *cheA1* and the *cheY1* mutants, despite an apparent similarity in the macroscopic floc structures. Collectively, these data indicate that disruption of the Che1 pathway is correlated with distinctive changes in the extracellular matrix, which likely result from changes in surface polysaccharides structure and/or composition.

Introduction

Azospirillum brasilense are soil diazotrophic bacteria that colonize the roots of many economically important grass and cereal species (Steenhoudt & Vanderleyden, 2000). Under conditions of high aeration and limiting availability of combined nitrogen, *A. brasilense* cells differentiate into aggregating cells and form dense flocs that are visible to the naked eye (Sadasivan & Neyra, 1985; Burdman *et al.*, 1998). Flocs are formed by cell-to-cell aggregation between non-motile cells embedded in a dense extracellular matrix (Burdman *et al.*, 2000b). Flocculation correlates with, and likely requires the production of, arabinose-rich exopolysaccharides (Bahat-Samet *et al.*, 2004). Scanning electron and

fluorescence microscopy studies of *A. brasilense* aggregating cells indicate the presence of fibrillar material connecting cells to each other or to biotic or abiotic substrates (Bashan *et al.*, 1986, 1991). These fibrils seem to be absent in nonaggregating cells or mutant strains that are defective in aggregation, suggesting that they may play a role in promoting this behavior (Burdman *et al.*, 1998; Skvortsov & Ignatov, 1998). The detailed biochemical composition of this fibrillar material remains unknown, although it is possible that it is related to exopolysaccharide production (Bahat-Samet *et al.*, 2004). In support of this idea, the degree of bacterial aggregation appears to correlate with the amount and composition of exopolysaccharide produced by several *A. brasilense* strains (Burdman *et al.*, 1998).

Chemotaxis is perhaps the most-studied signal transduction pathway in bacteria (reviewed in Sourjik, 2004; Wadhams & Armitage, 2004; Parkinson *et al.*, 2005; Hazelbauer *et al.*, 2008). Despite the identification of homologous chemotaxis systems in phylogenetically distant bacteria and archaeal species, there is a huge diversity in both the number of chemotaxis operons encoded within bacterial genomes and their physiological roles (Wadhams & Armitage, 2004). Recent studies have shown that the functions of chemotaxis-like pathways are not limited to the regulation of motility patterns, but also include the regulation of biofilm formation, exopolysaccharide production, and cell-to-cell interactions (Black & Yang, 2003; Hickman *et al.*, 2005; Yang & Li, 2005; Caiazza *et al.*, 2007). In prototypical chemotaxis, the histidine kinase CheA and the response regulator CheY form a two-component signal transduction system, which ultimately modulate the probability of changes in the direction of rotation of flagellar motors in response to specific environmental cues. Changes in the phosphorylation of CheY regulated by the CheA–CheY phosphorylation cascade modulate the affinity of CheY for the flagellar motor switch complex and thus chemotaxis. Surprisingly, in *A. brasilense*, strains carrying mutations in components of the Che1 chemotaxis-like pathway were found to be affected in their ability to interact by cell-to-cell aggregation and in flocculation. Mutant strains lacking functional CheA1 or CheY1 aggregate and flocculate significantly more than the wild-type strain, suggesting that Che1 modulates the ability of *A. brasilense* cells to flocculate. However, the exact mechanism by which the Che1 pathway regulates cellular functions other than chemotaxis is not known (Bible *et al.*, 2008). Initial attempts at identifying extracellular structures produced specifically by the mutant strains lacking CheA1 and CheY1 and thus controlled by the activity of Che1 have failed, but an effect of Che1 on exopolysaccharide production was suggested from differences in Congo Red staining of colonies (Bible *et al.*, 2008). Flocculation in *A. brasilense* has been correlated previously with changes in the structure and/or the composition of the extracellular matrix (reviewed in Burdman *et al.*, 2000b), and thus the current working hypothesis is that the Che1 pathway affects flocculation by modulating changes in the structure and/or the composition of the extracellular matrix (Bible *et al.*, 2008).

In this study, we tested this hypothesis by applying atomic force microscopy (AFM) techniques to investigate the cell surfaces of wild-type *A. brasilense* and its Che1 mutant strain derivatives [AB101 ($\Delta cheA1$) and AB102 ($\Delta cheY1$)]. AFM was selected because it allows nanoscale resolution of biological materials without prior sample fixation. Resolution limitations associated with optical imaging methods and the fixation and dehydration procedures typically associated with classical electron microscopy techniques

can inhibit visualization of extracellular structures and could have prevented the identification of CheA1- or CheY1-specific extracellular structures produced during flocculation (Dufrene, 2002, 2003; Bible *et al.*, 2008). The data obtained using AFM conclusively identify a distinctive remodeling of the extracellular matrix, likely via changes in exopolysaccharide production, in AB101 ($\Delta cheA1$) and AB102 ($\Delta cheY1$) under flocculation conditions as well as remarkable differences in the structural organization of the aggregates formed by each of these two strains. Further analyses using a lectin-binding assay, flocculation inhibition, and comparison of lipopolysaccharides profiles are consistent with the hypothesis that the Che1 pathway modulates changes in the extracellular matrix that coincide with flocculation, although this effect is likely to be indirect because our data reveal distinct changes in the content or the organization of the extracellular matrix of the $\Delta cheA1$ and $\Delta cheY1$ mutant strains.

Materials and methods

Strains and growth conditions

Azospirillum brasilense wild-type parental strain Sp7 (ATCC29145) and mutant strains defective in CheA1 [AB101 ($\Delta cheA1$)] and CheY1 [AB102 ($\Delta cheY1$)] were used in this study (Stephens *et al.*, 2006; Bible *et al.*, 2008). Strains were grown in nutrient tryptone–yeast extract (TY) and a minimal salt medium (MMAB) (Hauwaerts *et al.*, 2002). To induce flocculation, cells were grown in 20-mL glass culture tubes with 5 mL of flocculation media (MMAB with 20 mM malate and 0.5 mM NaNO₃). Cultures were inoculated with 250 μ L of an overnight culture normalized to an OD_{600 nm} of 1.0 (approximately 10⁶ CFU mL⁻¹ for all strains), and incubated on a platform shaker (200 r.p.m.) at 28 °C for 24 h or 1 week.

Quantification of flocculation

To quantify flocculation, we modified a protocol described previously (Madi & Henis, 1989; Burdman *et al.*, 1998). Briefly, 1 mL of sample was subjected to mild sonication using a Branson Digital Sonifer Model 102C equipped with a 3.2 mm tapered micro tip. Settings for sonication included sonic pulses of 2 s on and 2 s off, with the amplitude set at 10%. The percentage of flocculation was calculated by $(OD_a - OD_b / OD_a) \times 100$, where OD_a is the OD after sonication and OD_b the OD before sonication.

AFM imaging

AFM samples were prepared as described, with slight modifications (Doktycz *et al.*, 2003). Briefly, 1-mL aliquots of bacteria were harvested by centrifugation (6000 g) after

24 h or 1 week of growth. Cells were resuspended in 100 μL dH_2O and then deposited on a freshly cleaved mica surface. Samples were air-dried 8–24 h before imaging with a Pico-Plus atomic force microscope (Agilent Technologies, Tempe, AZ) using a 100 μm multipurpose scanner. The instrument was operated in the contact mode at 512 pixels per line scan with speeds ranging from 0.5 to 1.0 Hz. A Veeco MLCT-E cantilever with a nominal spring constant of 0.5 N m^{-1} was used for imaging. For all samples, first-order flattened topography and deflection scans were acquired with sizes ranging from 1.5 to 75 μm .

Lectin-binding assay

Strains were grown in 5 mL cultures as described above. After 24 h, cells were stained with Syto61 (Invitrogen) following the manufacturer's instructions and resuspended in 200 μL phosphate-buffered saline (PBS) (pH 7.4). Fluorescein isothiocyanate (FITC)-conjugated lentil (LcH; Sigma #L9262) or lima bean lectins (LBL; Sigma #L0264) were added at a final concentration of $50 \mu\text{g mL}^{-1}$. The cells were incubated at room temperature with shaking for 20 min, harvested at 8000 r.p.m., and washed with PBS. A Leica TCS SP2 scanning confocal microscope was used for image acquisition. IMAGEJ was used for image analysis.

Flocculation inhibition assay

An aggregation bioassay described previously (Burdman *et al.*, 1999, 2000a) was used to assess the roles of D-glucose and L-arabinose in flocculation. Briefly, all strains were grown in flocculation medium or in MMAB. After 24 h, flocculating cultures were sonicated for 20 s and then centrifuged (16 000 g, 2 min). The supernatant was then added to cells grown in MMAB (nonflocculating) along with 0.05, 0.1, or 0.5 M concentrations of D-glucose or L-arabinose. The cultures were incubated at 28°C with shaking for 3–4 h. Flocculation was quantified using the protocol described above.

Extraction of lipopolysaccharides

Lipopolysaccharides was extracted from all strains grown in TY and flocculation medium at 24 h and 1 week using an lipopolysaccharides extraction Kit (Intron Biotechnology) following the manufacturer's instructions. Equal aliquots of lipopolysaccharides extract were dissolved in sodium dodecyl sulfate (SDS) sample buffer, boiled for 5 min, and loaded onto a 4–20% Tris-HCl SDS-polyacrylamide gel electrophoresis gel (Bio-Rad). Samples were electrophoresed at 150 V for 1 h. Gels were silver stained as described (Kittelberger & Hilbink, 1993).

Results

Flocculation

Consistent with previous work, we observed differences in the flocculation behavior of *A. brasilense* strains deficient in CheA1 and CheY1 compared with wild-type cells (Table 1). At 24 h, aggregative structures and flocs were visible for the Che1 pathway mutant strains AB101 (ΔcheA1) and AB102 (ΔcheY1), but were not seen in the wild-type cultures at this time point. The amount of flocculation relative to planktonic cells for AB101 and AB102 was increased after 1 week of incubation (Table 1). Flocculation was significant for the wild-type culture after 1 week of incubation (Table 1). All strains had similar motility before flocculation, and all strains lost motility after significant flocculation occurred, in agreement with previous findings (Burdman *et al.*, 1998; Pereg Gerck *et al.*, 2000; Bible *et al.*, 2008). Taken together, these data are consistent with earlier findings that AB101 and AB102 flocculate earlier than the wild-type strain (Bible *et al.*, 2008).

Comparison of extracellular matrix structures by AFM

Examination of AFM images revealed that the extracellular matrix of AB101 (ΔcheA1) and AB102 (ΔcheY1) contained fibrillar material at 24 h (Fig. 1c and d and Supporting Information, Fig. S1). The extracellular matrix of AB101 (ΔcheA1) and AB102 (ΔcheY1) appeared as a ridged structure on the surface of cells with fibrils protruding from the cells (Fig. 1c and d, Fig. S1). In contrast, the extracellular material surrounding cells of the nonflocculating wild-type strain appeared to be smooth and globular at 24 h (Fig. 1a). Numerous high-resolution scans of wild-type nonflocculating cells failed to reveal fibrillar material (Fig. 1a and data not shown). After 1 week, however, fibrillar material was observed for flocculating wild-type cells (Fig. 1b).

Despite the apparent similarity of the macroscopic flocculation phenotype of the mutant strains, analyses of AFM topography and deflection images revealed a dissimilarity in the organizational pattern of the aggregating cells (Figs 2 and S2). The most striking difference was observed in comparing the extracellular material of AB102 (ΔcheY1) with that of AB101 (ΔcheA1) or wild-type cells. A network

Table 1. Quantification of flocculation

Strains	Percent aggregation	
	24 h	1 week
Wild-type Sp7	0.01 ± 0.67	32.3 ± 9.50
AB101 (ΔcheA1)	52.0 ± 0.07	95.0 ± 0.61
AB102 (ΔcheY1)	86.3 ± 0.02	93.5 ± 0.38

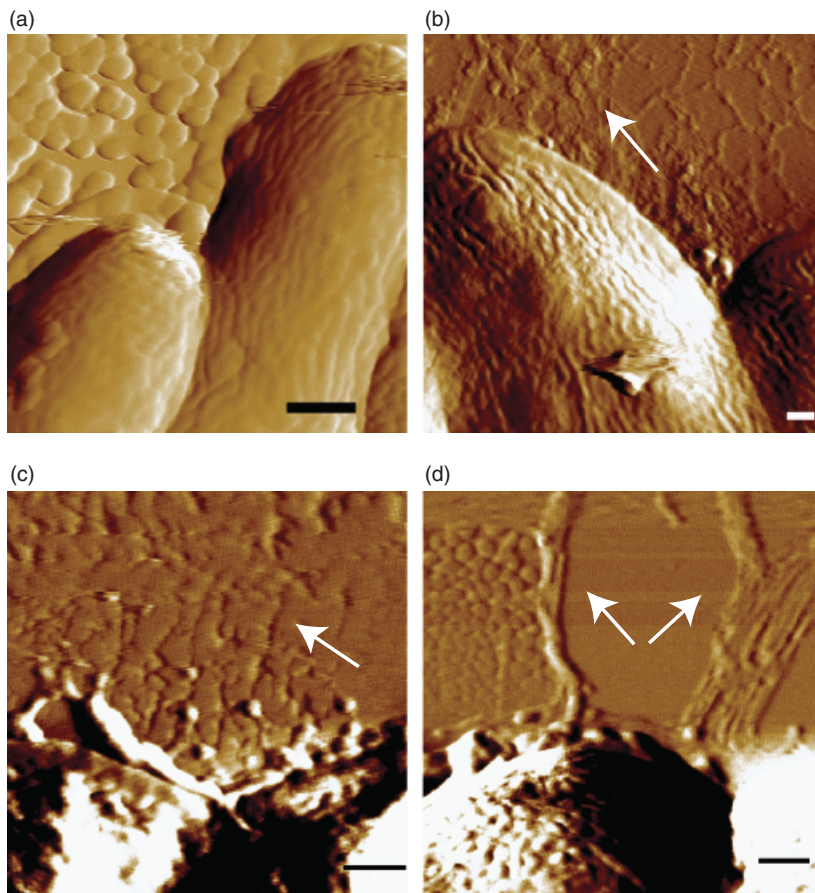


Fig. 1. Flocculating *che1* mutants produce a fibrillar material during premature flocculation. (a) Nonflocculating wild-type Sp7 at 24 h; (b) flocculating wild-type Sp7 at 1 week; (c) flocculating mutant strain AB101 ($\Delta cheA1$) at 24 h; (d) flocculating mutant strain AB102 ($\Delta cheY1$) at 24 h. The white arrows point to the fibrillar material. All scale bars represent 200 nm.

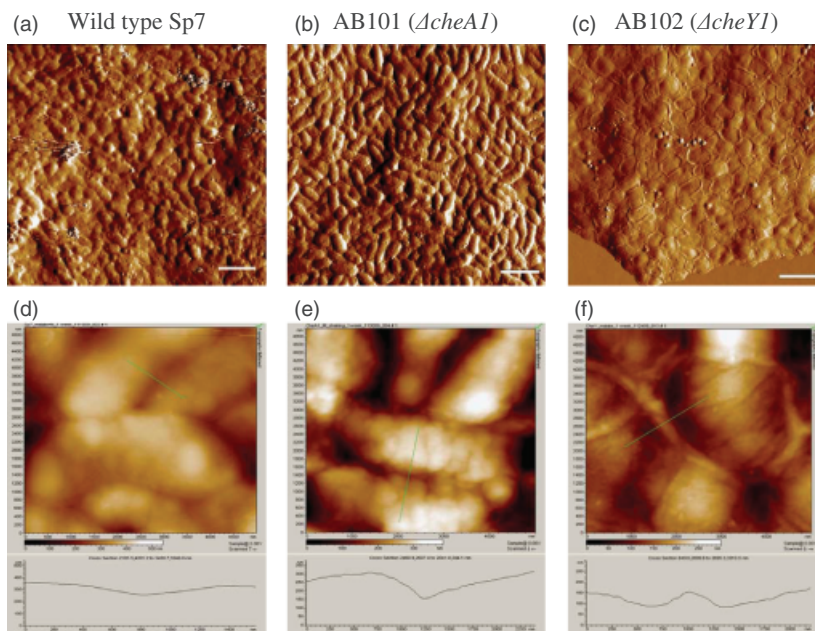


Fig. 2. AFM deflection images revealed a dissimilarity in the organization of flocs between the two mutant strains. (a) Wild-type Sp7 deflection; (b) AB101 ($\Delta cheA1$) deflection; (c) AB102 ($\Delta cheY1$) deflection; (d) $5 \mu\text{m}^2$ micrograph with a height cross-section measurement between wild-type cells; (e) between AB101 ($\Delta cheA1$) cells; and (f) between AB102 ($\Delta cheY1$) cells revealing a distinct extracellular material not observed for wild type or AB101 ($\Delta cheA1$). Scale bars represent $5 \mu\text{m}$.

of extracellular material is visible between the AB102 ($\Delta cheY1$) cells as early as 24 h (data not shown) and it becomes more distinct after 1 week (Fig. 2c). Line scans across the flocs indicate that AB102 ($\Delta cheY1$) cells are embedded in a matrix that spans approximately 400 nm between cells (Fig. 2f). This tight organization is not observed in flocs formed by AB101 ($\Delta cheA1$) (Fig. 2b). In this strain, as well as in flocculating wild-type cells, individual cells are distinctly defined within the flocs and no obvious features are observed between the cells (Fig. 2a, b, d, and e)

Flocculation inhibition assay

Given the noticeable difference in the floc structures discovered using AFM techniques, we sought to use a flocculation inhibition assay to determine whether glucose and/or arabinose residues, previously shown to contribute to flocculation in *A. brasilense* (Burdman *et al.*, 2000a), were present and participated in cell-to-cell aggregation and flocculation. The addition of 0.5 M arabinose to flocculating cultures of both mutant strains caused a significant reduction in the total amount of flocculation (Fig. 3a), suggesting that arabinose contributes to the structure and/or the stability of the flocs formed by these strains. In addition, we found that flocs of the AB102 ($\Delta cheY1$) strain were significantly more sensitive to the competitive addition of exogenous arabinose (Fig. 3a) than the flocs of AB101. Similarly, high concentrations of glucose (0.5 M) reduced flocculation in both mutant strains and flocs formed by the AB102 ($\Delta cheY1$) strain appeared to be more sensitive to the addition of glucose, with almost complete inhibition of flocculation after the addition of 0.5 M glucose (Fig. 3b).

Lectin-binding assay

To further investigate differences in the extracellular matrix, we used FITC-conjugated lentil lectin (LcH) (affinity for α -mannose and α -glucose) and lima bean lectin (LBL) (affinity for *N*-acetyl galactosamine) to probe for specific carbohydrates present on or around the cell surface. Wild-type cells did not show any significant binding of either lectin after 24 h of growth as determined by fluorescence imaging and statistical analysis (Fig. 4; Table S1). Both lectins were found to stain AB101 ($\Delta cheA1$) cells and the surrounding material (Fig. 4b and h). In comparison with AB101, AB102 ($\Delta cheY1$) cells displayed reduced staining by both lectins (Fig. 4c and i). When normalized to the fluorescence signal of Syto61 that stains all cells (Fig. 4d–f and j–l), the lectin fluorescence signal detected for AB102 ($\Delta cheY1$) floc structures was significantly ($P = 0.05$) reduced for both lectins with respect to AB101 (Table S1).

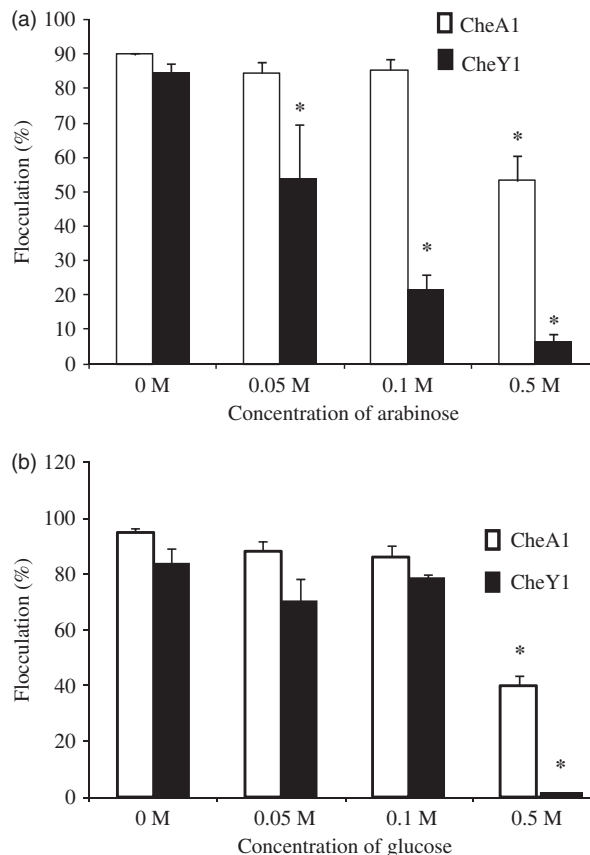


Fig. 3. The effect of L-arabinose (a) and D-glucose (b) on flocculation for *che1* mutants. The data in both (a) and (b) represent the average of three replicates for one representative experiment per strain. The asterisks represent significant differences in binding inhibition between the monosaccharide treated cultures as analyzed by one- and two-way ANOVA ($P = 0.05$).

Lipopolysaccharides profiles of the Che1 mutants

The lipopolysaccharides profiles of the mutant and wild-type strains grown under flocculating and nonflocculating conditions were compared. Under conditions of growth in rich medium (TY), all strains had similar lipopolysaccharides profiles (Fig. 5). Differences in lipopolysaccharides profiles were detected between the strains as early as 24 h of incubation in flocculation medium, which corresponds to the time at which both mutant strains, but not the wild-type strain, flocculate. Under these conditions and compared with the lipopolysaccharides profile of the wild-type strain, a low-molecular-weight band (arrow 2, Fig. 5) is absent from the profile of both mutant strains while another low-molecular-weight band (arrow 3, Fig. 5) is significantly reduced. A higher molecular weight band (Fig. 5, arrow 1) is also clearly visible for all strains, but more abundant in the lipopolysaccharides profile of both mutant strains at 24 h.

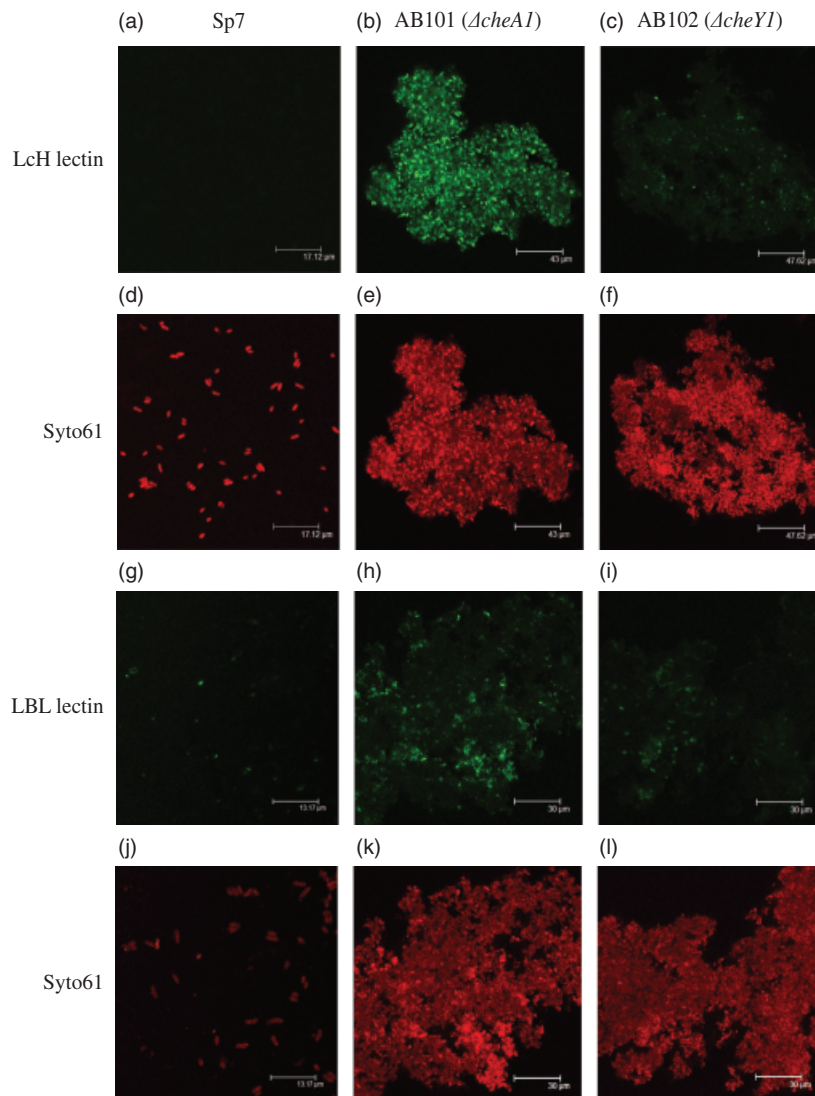


Fig. 4. The *che1* mutants differentially bind lentil (LcH) and lima bean (LBL) lectins. (a,d) wild-type stained with LcH and Syto61; (b,e) AB101 ($\Delta cheA1$) stained with LcH and Syto61; (c,f) AB102 ($\Delta cheY1$) stained with LcH and Syto61; (g,j) wild-type stained with LBL and Syto61; (h,k) AB101 ($\Delta cheA1$) stained with LBL and Syto61; (i,l) AB102 ($\Delta cheY1$) stained with LBL and Syto61..

After 1 week of incubation, the wild-type strain flocculated and its lipopolysaccharides profile mirrored that of the flocculated mutant strains: the lower molecular weight bands (arrows 2 and 3, Fig. 5) are significantly fainter while a higher molecular weight band (arrow 1, Fig. 5) shows an increase in relative abundance. Collectively, the data suggest that changes in the lipopolysaccharides profiles of flocculated cells are comparable for all strains, and that changes in lipopolysaccharides profiles are correlated and coincident with flocculation.

Discussion

In this study, we used high-resolution imaging to investigate the cell surface and the surrounding matrix of the *A. brasilense* AB101 ($\Delta cheA1$) and AB102 ($\Delta cheY1$) mutant cells during flocculation. Several recent investigations

support the hypothesis that exopolysaccharides and outer membrane proteins are involved in cell-to-cell aggregation leading to flocculation in *Azospirillum* spp. These data support a model in which flocculation is accompanied and perhaps triggered by several changes in cell surface properties, because flocculation coincides with remodeling of the cell surface and the extracellular matrix in *A. brasilense* (Delgallo *et al.*, 1989; Burdman *et al.*, 2000a; Bahat-Samet *et al.*, 2004; Mora *et al.*, 2008; Mulyukin *et al.*, 2009). Comparisons between AFM micrographs, lectin-binding affinities, and lipopolysaccharides profiles of planktonic and flocculating cells performed in the present study are consistent with this model because they collectively show that an increased flocculation phenotype correlates with a set of changes in cell surface characteristics, including the apparent specific production of fibrillar extracellular material at the edge of floc structures. Such fibrillar material was

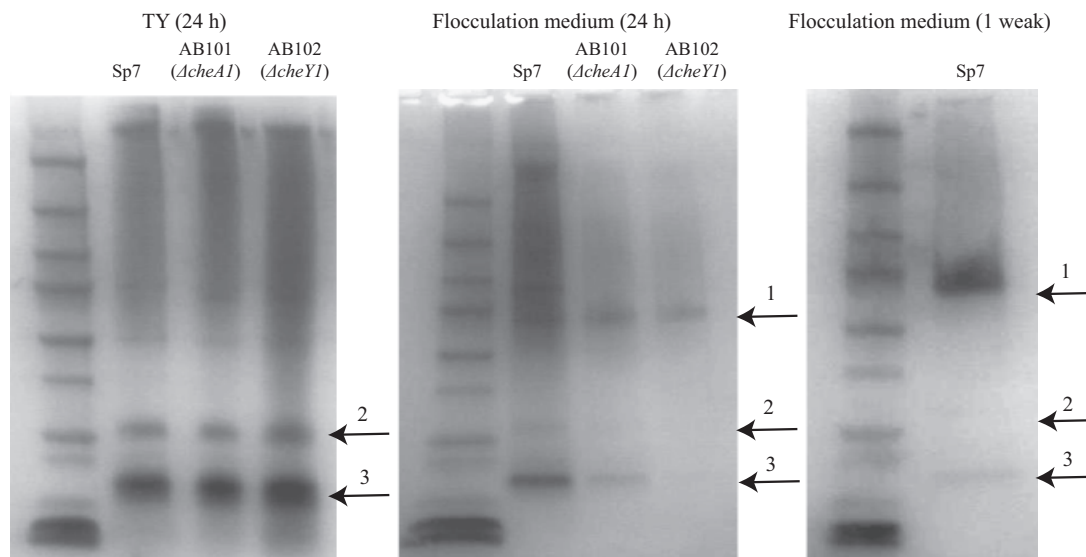


Fig. 5. Lipopolysaccharides profile of wild-type Sp7 and mutant strains grown in nutrient TY and flocculation medium. Arrows indicate the bands discussed in the text.

observed in all flocculated strains [AB101 ($\Delta cheA1$) and AB102 ($\Delta cheY1$) at 24 h and in the wild type at 1 week]. Furthermore, more abundant fibrillar material was detected on the surface of the AB102 ($\Delta cheY1$) strain, which correlates with the greater amount of flocculation observed consistently for this strain. Whether this fibrillar material associated with flocculating cells is directly related to or has a role similar to that of the fibrillar structures reportedly formed by *A. brasilense* Cd cells during aggregative attachment to wheat roots and sand particles remains to be determined (Bashan *et al.*, 1991).

The function of the chemotaxis-like Che1 pathway in modulating flocculation in *A. brasilense* is unexpected and the underlying molecular mechanism(s) remains to be determined. However, several other chemotaxis-like signal transduction pathways regulate functions other than motility by mechanisms that are yet to be determined (Black & Yang, 2003; Berleman & Bauer, 2005a, b; Hickman *et al.*, 2005). Data obtained here shed light on several important features of Che1-dependent regulation of flocculation behavior in *A. brasilense*. If the signaling output of the Che1 pathway, in which CheA1 and CheY1 are expected to form a chemotaxis-like two-component system (Hauwaerts *et al.*, 2002; Stephens *et al.*, 2006; Bible *et al.*, 2008), is the direct regulation of molecular target(s) modulating the flocculation behavior, then mutations that impair CheA1 or CheY1 functions should yield similar phenotypes. This study revealed several distinguishing features of the flocs formed by each of the mutant strains that are not consistent with a direct function of Che1 in the regulation of flocculation. First, although cells of both mutant strains were adherent and embedded in a complex matrix apparently comprised of

fibrillar material, cell-to-cell contacts within the matrix of the AB102 ($\Delta cheY1$) strain were separated by a thick layer that was visible by AFM after 1 week. This layer formed a tight network around each individual cell within the floc. In contrast, in the flocs of AB101 ($\Delta cheA1$), individual cells were distinctly defined and no obvious connecting features were observed between the cells.

Because it is impossible to determine the composition of this material from imaging alone, we used flocculation inhibition and lectin-binding assays to analyze the different structures observed between the two strains in more detail. The results of the lectin-binding assay suggest that AB101 ($\Delta cheA1$) produces an exopolysaccharide that is more abundant in α -mannose and/or α -glucose, and *N*-acetyl galactosamine than the exopolysaccharide produced by AB102 ($\Delta cheY1$). Previous studies have shown that the glucose content of exopolysaccharide is significantly lower during flocculation in the wild-type Sp7 strain and in other mutant derivative strains with increased aggregation capacity (Bahat-Samet *et al.*, 2004). Consistent with these data, AB102 ($\Delta cheY1$) strain displays a stronger flocculation phenotype and its extracellular matrix appears to have a reduced mannose and/or a glucose content relative to that of AB101 ($\Delta cheA1$). An alternative explanation for these data is that the structural organization of the AB102 ($\Delta cheY1$) floc reduces the accessibility of the sugar residues to the lectin, thus limiting the amount of lectin that binds to the cells and the surrounding matrix.

Even though the floc structures of the two mutant strains showed different binding affinities for lectins, indicating possible differences in the polysaccharide composition of the exopolysaccharide produced during flocculation, these

results do not necessarily demonstrate the contribution of specific polysaccharides to aggregation or flocculation. Previous studies showed that exopolysaccharide composition is modified over time from a glucose-rich exopolysaccharide to an arabinose-rich exopolysaccharide and that this temporal change correlates directly with the timing of flocculation (Bahat-Samet *et al.*, 2004). In agreement with this observation, flocs formed by the $\Delta cheY1$ mutant were more sensitive to the addition of arabinose in the flocculation inhibition assay, suggesting that the sugar residues comprising the matrix of these strains are different in structure and/or composition. This could also suggest that the $\Delta cheY1$ strain, which flocculates quantitatively more, represents a more advanced stage of flocculation compared with the $\Delta cheA1$ mutant strain or the wild-type strain. Comparison of changes in the lipopolysaccharides profiles of the wild-type and mutant strains lends further credence to this possibility because differences in the lipopolysaccharides profiles were seen to occur for all strains, but at different times during the flocculation process. Therefore, the mutant strains lacking *cheA1* or *cheY1* may be affected in the timing of flocculation, which may result, for example, from an increased sensitivity of the cells to the cues that trigger flocculation or perhaps to other effects. Structural and other differences identified between the flocs formed by $\Delta cheA1$ and $\Delta cheY1$ strains thus collectively suggest that the function of Che1 in modulating flocculation is indirect. Taken together and with data from the literature (Burdman *et al.*, 2000a; Bahat-Samet *et al.*, 2004; Bible *et al.*, 2008), the results obtained here underscore the significant changes of the cell surface and extracellular matrix that occur during flocculation and support a model in which flocculation in *A. brasilense* is an adaptive behavior that allows the cells to differentiate into resistant forms via extensive remodeling of the cell surface and the extracellular matrix, including lipopolysaccharides and exopolysaccharide.

Acknowledgements

The authors would like to thank Dave Allison for helpful discussions. This research was funded by the Genomic Science Program of the Office of Biological and Environmental Research, US DOE, and NSF MCB-0919819 to G.A. Oak Ridge National Laboratory is managed by UT-Battelle, LLC, for the US Department of Energy under Contract no. DE-AC05-00OR22725.

Authors' contribution

A.N.E. and P.S. contributed equally to this work.

References

- Bahat-Samet E, Castro-Sowinski S & Okon Y (2004) Arabinose content of extracellular polysaccharide plays a role in cell aggregation of *Azospirillum brasilense*. *FEMS Microbiol Lett* **237**: 195–203.
- Bashan Y, Levanony H & Klein E (1986) Evidence for a weak active external adsorption of *Azospirillum brasilense* Cd to wheat roots. *J Gen Microbiol* **132**: 3069–3073.
- Bashan Y, Mitiku G, Whitmoyer RE & Levanony H (1991) Evidence that fibrillar anchoring is essential for *Azospirillum brasilense* Cd attachment to sand. *Plant Soil* **132**: 73–83.
- Berleman JE & Bauer CE (2005a) Involvement of a Che-like signal transduction cascade in regulating cyst cell development in *Rhodospirillum centenum*. *Mol Microbiol* **56**: 1457–1466.
- Berleman JE & Bauer CE (2005b) A che-like signal transduction cascade involved in controlling flagella biosynthesis in *Rhodospirillum centenum*. *Mol Microbiol* **55**: 1390–1402.
- Bible AN, Stephens BB, Ortega DR, Xie Z & Alexandre G (2008) Function of a chemotaxis-like signal transduction pathway in modulating motility, cell clumping, and cell length in the alphaproteobacterium *Azospirillum brasilense*. *J Bacteriol* **190**: 6365–6375.
- Black WP & Yang Z (2003) *Myxococcus xanthus* chemotaxis homologs DifD and DifG negatively regulate fibril polysaccharide production. *J Bacteriol* **186**: 1001–1008.
- Burdman S, Jurkevitch E, Schwartzburd B, Hampel M & Okon Y (1998) Aggregation in *Azospirillum brasilense*: effects of chemical and physical factors and involvement of extracellular components. *Microbiology* **144**: 1989–1999.
- Burdman S, Jurkevitch E, Schwartzburd B & Okon Y (1999) Involvement of outer-membrane proteins in the aggregation of *Azospirillum brasilense*. *Microbiology* **145**: 1145–1152.
- Burdman S, Jurkevitch E, Soria-Diaz ME, Serrano AM & Okon Y (2000a) Extracellular polysaccharide composition of *Azospirillum brasilense* and its relation with cell aggregation. *FEMS Microbiol Lett* **189**: 259–264.
- Burdman S, Okon Y & Jurkevitch E (2000b) Surface characteristics of *Azospirillum brasilense* in relation to cell aggregation and attachment to plant roots. *Crit Rev Microbiol* **26**: 91–110.
- Caiazza NC, Merritt JH, Brothers KM & O'Toole GA (2007) Inverse regulation of biofilm formation and swarming motility by *Pseudomonas aeruginosa* PA14. *J Bacteriol* **189**: 3603–3612.
- Delgallo M, Negi M & Neyra CA (1989) Calcofluor-binding and lectin-binding exocellular polysaccharides of *Azospirillum brasilense* and *Azospirillum lipoferum*. *J Bacteriol* **171**: 3504–3510.
- Doktycz MJ, Sullivan CJ, Hoyt PR, Pelletier DA, Wu S & Allison DP (2003) AFM imaging of bacteria in liquid media immobilized on gelatin coated mica surfaces. *Ultramicroscopy* **97**: 209–216.
- Dufrene YF (2002) Atomic force microscopy, a powerful tool in microbiology. *J Bacteriol* **184**: 5205–5213.

- Dufrene YF (2003) Recent progress in the application of atomic force microscopy imaging and force spectroscopy to microbiology. *Curr Opin Microbiol* **6**: 317–323.
- Hauwaerts D, Alexandre G, Das SK, Vanderleyden J & Zhulin IB (2002) A major chemotaxis gene cluster in *Azospirillum brasilense* and relationships between chemotaxis operons in alpha-proteobacteria. *FEMS Microbiol Lett* **208**: 61–67.
- Hazelbauer GL, Falke JJ & Parkinson JS (2008) Bacterial chemoreceptors: high-performance signaling in networked arrays. *Trends Biochem Sci* **33**: 9–19.
- Hickman JW, Tifrea DF & Harwood CS (2005) A chemosensory system that regulates biofilm formation through modulation of cyclic diguanylate levels. *P Natl Acad Sci USA* **102**: 14422–14427.
- Kittelberger R & Hilbink F (1993) Sensitive silver-staining detection of bacterial lipopolysaccharides in polyacrylamide gels. *J Biochem Biophys Meth* **26**: 81–86.
- Madi L & Henis Y (1989) Aggregation in *Azospirillum brasilense* Cd – conditions and factors involved in cell-to-cell adhesion. *Plant Soil* **115**: 89–98.
- Mora P, Rosconi F, Fraguas LF & Castro-Sowinski S (2008) *Azospirillum brasilense* Sp7 produces an outer-membrane lectin that specifically binds to surface-exposed extracellular polysaccharide produced by the bacterium. *Arch Microbiol* **189**: 519–524.
- Mulyukin AL, Suzina NE, Pogorelova AY, Antonyuk LP, Duda VI & El-Registan GI (2009) Diverse morphological types of dormant cells and conditions for their formation in *Azospirillum brasilense*. *Microbiology* **78**: 33–41.
- Parkinson JS, Ames P & Studdert CA (2005) Collaborative signaling by bacterial chemoreceptors. *Curr Opin Microbiol* **8**: 116–121.
- Pereg Gerk L, Gilchrist K & Kennedy IR (2000) Mutants with enhanced nitrogenase activity in hydroponic *Azospirillum brasilense*–wheat associations. *Appl Environ Microb* **66**: 2175–2184.
- Sadasivan L & Neyra CA (1985) Flocculation in *Azospirillum brasilense* and *Azospirillum lipoferum* – exopolysaccharides and cyst formation. *J Bacteriol* **163**: 716–723.
- Skvortsov IM & Ignatov VV (1998) Extracellular polysaccharides and polysaccharide-containing biopolymers from *Azospirillum* species: properties and the possible role in interaction with plant roots. *FEMS Microbiol Lett* **165**: 223–229.
- Sourjik V (2004) Receptor clustering and signal processing in *E. coli* chemotaxis. *Trends Microbiol* **12**: 569–576.
- Steenhoudt O & Vanderleyden J (2000) *Azospirillum*, a free-living nitrogen-fixing bacterium closely associated with grasses: genetic, biochemical and ecological aspects. *FEMS Microbiol Rev* **24**: 487–506.
- Stephens BB, Loar SN & Alexandre G (2006) Role of CheB and CheR in the complex chemotactic and aerotactic pathway of *Azospirillum brasilense*. *J Bacteriol* **188**: 4759–4768.
- Wadhams GH & Armitage JP (2004) Making sense of it all: bacterial chemotaxis. *Nat Rev Mol Cell Bio* **5**: 1024–1037.
- Yang ZM & Li Z (2005) Demonstration of interactions among *Myxococcus xanthus* Dif chemotaxis-like proteins by the yeast two-hybrid system. *Arch Microbiol* **183**: 243–252.

Supporting Information

Additional Supporting Information may be found in the online version of this article:

Fig. S1. AFM $5 \times 5 \mu\text{m}$ deflection scans of wild-type and mutant strains.

Fig. S2. AFM topography images of (a) wild-type Sp7; (b) AB101 (ΔcheA1); (c) AB102 (ΔcheY1).

Table S1. Quantification of lectin binding.

Please note: Wiley-Blackwell is not responsible for the content or functionality of any supporting materials supplied by the authors. Any queries (other than missing material) should be directed to the corresponding author for the article.